J Appl Electrochem (2009) 39:955–960
DOI 10.1007/s10800-009-9780-y

REVIEW ARTICLE

Electrolyte optimization for a Li ion battery by charge profile analysis

Minwhan Cha · Cheolsoo Jung

Received: 11 March 2008 / Accepted: 23 December 2008 / Published online: 19 January 2009

Abstract Electrolyte design for Li ion batteries was approached by means of comparison of faradaic and non-faradaic currents. The faradaic current by the movement of Li^+ ions was dependent on the composition of the electrolyte and was related to the battery capacity; the higher the capacity, the greater the current by the faradaic reaction. The open circuit potential of the electrode with a greater faradaic current decreased at a slower rate than that of the electrode with a smaller faradaic current. This analysis method can be used to prepare an optimal electrolyte of an actual Li ion battery, especially when developing batteries with excellent high-rate discharge capabilities and low temperature discharge properties.

Keywords Faradaic reaction · Non-faradaic reaction · Open circuit voltage · Li ion battery · Electrolyte

1 Introduction

The energy state of a rechargeable battery is determined by estimating the difference between the electrical potentials of its cathode and anode. In the case of a Li ion battery, this difference is controlled by graphite and $LiMO_2$ (M=Co, Mn, Ni) electrodes, which intercalate and dissociate lithium during the charging period. The electrolyte stability at the surface of the electrode changes with the state of charge of the electrodes. Therefore, analyzing the electrochemical behavior at the surface of the electrode is the key towards stabilizing a Li ion battery. Various studies have been conducted to increase the stability of the Li ion battery by manipulating the electrolyte components (solvent, salt and additive) to prevent the decomposition of the electrolyte by oxidation and reduction on the surface of the charged electrodes [1–7]. These studies have made a significant contribution towards increasing the safety of the Li ion battery in view of continuous upgrades and escalating demands of technology.

In general, faradaic current is defined as the transfer of an electron across the interface between the electrode and electrolyte; this current is responsible for the electrochemical reduction or oxidation of the electrolyte at the interface. Non-faradaic current is defined as the accumulation of charge at the metal-solution interface; this current is responsible for the formation of an electrical double layer [8]. The formation of this double layer depends on the composition of the electrolyte and the potential applied to the electrode. In the Li ion battery, since the formation of the electrical double layer during the initial charging period does not significantly depend on the battery capacity, non-faradaic currents are seldom used to generate analytical signals. However, electric potential is determined by the summation of the faradaic and non-faradaic potentials estimated during the charging and discharging periods, respectively. The non-faradaic potential is determined from a capacitive component, and it is related to the electrochemical stability between the electrode and electrolyte. On the other hand, the faradaic potential is determined not only from the electrochemical reactions of the electrolyte components on the surface of the electrode but also from the intercalation and dissociation of Li^+ ions into and out of the electrode in the Li ion battery. Xu et al. proposed that the actual electrode should be used for the electrochemical reaction, because the faradaic reaction depends on the surface of the electrode [1]. However, they did not

M. Cha · C. Jung (✉)
Department of Chemical Engineering, University of Seoul,
13 Shiripdae-gil, Dongdaemun-gu, Seoul 130-743, Korea
e-mail: csjung@uos.ac.kr

sufficiently discuss the dissociating and intercalating reactions of Li^+ ions in the faradaic process, even though the ions dissociate from the $LiMO_2$ electrode by oxidation and intercalate to the graphite electrode by reduction during the charging period. In this paper, the faradaic and non-faradaic reactions during the charging period of the graphite and $LiCoO_2$ electrodes were compared to optimize the composition of the electrolyte for an actual Li ion battery, by using linear sweep voltage (LSV) and open circuit potential measurement (OCP). All electrochemical analyses were performed using a scanning electrochemical microscope (SECM) placed in an argon-charged glove box to measure the currents (in pA) precisely.

2 Experimental

Electrolyte grade ethylene carbonate (EC), diethyl carbonate (DEC), ethyl methyl carbonate (EMC), dimethyl carbonate (DMC), and lithium salts ($LiPF_6$, $LiBF_4$, and LiTFSI [TFSI = *bis*(trifluoromethane sulfonylimide)] were obtained from Cheil Co., Ltd. and used without further purification. Graphite and $LiCoO_2$ electrodes were obtained from Enerland Co., Ltd. as the mass-producing grade for a Li ion battery. Electrolyte systems were prepared by volume ratio in a glove box filled with argon gas (purity 99.99%). All the electrochemical reactions were analyzed using a scanning electrochemical microscope (SECM, CHI900B, CH instruments) installed in the glove box. A Pt wire was used as a reference electrode; graphite and $LiCoO_2$ were alternately used as working and counter electrodes. The radius of the working electrodes—graphite and $LiCoO_2$—was 3.22 mm, and the potential difference between $LiCoO_2$ and graphite was almost 0 V in the uncharged state. The charging rate for the reduction and oxidation of the graphite and $LiCoO_2$ electrodes, respectively, was fixed at 50 mV s^{-1}. All data for the reduction of the graphite electrode and the oxidation of the $LiCoO_2$ electrode were obtained separately during the first charging process.

3 Results and discussion

3.1 Oxidation and reduction behavior of $LiCoO_2$ and graphite

The electrochemical reaction comprises the faradaic and non-faradaic reactions that occur at the interface between the electrode and electrolyte. In the Li ion battery, the faradaic reaction comprises the decomposition of the electrolyte and the movement of Li^+ ions during charging and discharging processes. Of these reactions, the decomposition of the electrolyte is an ancillary reaction that depends on the change in the electrode potential and mainly occurs during the initial charging period at the graphite electrode or during the overcharging period at the $LiCoO_2$ electrode. The movement of Li^+ ions is derived from the association-disassociation in the $LiCoO_2$ electrode and intercalation–deintercalation in the graphite electrode. The non-faradaic reaction is responsible for the electrochemical stability of the electrolyte. Fig. 1 shows the total LSV data obtained in terms of the reduction at the graphite electrode and the oxidation at the $LiCoO_2$ electrode, with the electrolyte having a $LiPF_6$ concentration of 0.5–2.0 mol L^{-1} in EC. The predominant difference between the reduction and oxidation processes was that the non-faradaic region on the $LiCoO_2$ substrate was shorter than that on the graphite substrate. The potential of the non-faradaic region ranged from 0 to +0.5 V for $LiCoO_2$ and from 0 to –1.9 V for graphite; therefore, the potential window of the electrolyte required for resisting the cathodic reaction must be wider than that required for resisting the anodic reaction. In the case of the graphite electrode, the peak at −2.2 V is thought to occur due to the formation of a solid electrolyte interface (SEI) layer. However, in the case of the $LiCoO_2$ electrode, it was difficult to observe the special peak of the oxidation current above of +0.5 V, which is the potential at which Li^+ dissociation begins. Therefore, it is clear that decomposition of the electrolyte during the initial charging period is governed by the reduction at the graphite electrode, not by oxidation at the $LiCoO_2$ electrode. According to Aurbach and Andersson, the reason for such a phenomenon is that all the cathode materials—transition metal oxide based on Co, Mn, and Ni—are already in an oxidized state; therefore, they cannot be oxidized further [9–12]. However, it is reported that a protective film is formed on $LiMO_2$ compounds such as $LiMnO_2$, $LiCoO_2$, and $LiNiO_2$ at high oxidation potentials;

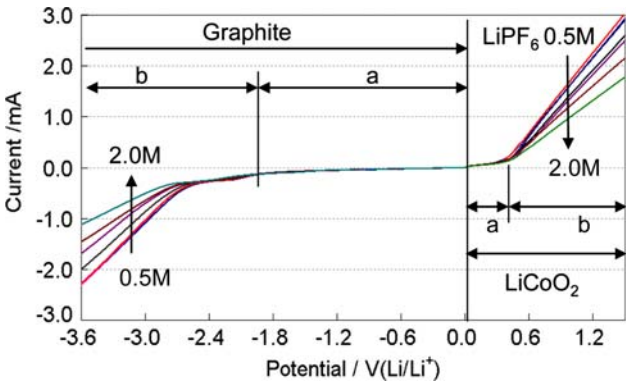

Fig. 1 Total LSV data of reduction process at the graphite electrode and of the oxidation process at the $LiCoO_2$ electrode with $LiPF_6$ contents from 0.5 to 2.0 mol L^{-1} in EC: **a** non-faradaic region, **b** faradaic region

this affects the irreversible capacity of the Li ion battery [13–17]. These oxidation films are analyzed by determining the impedance, surface image and surface structure of the electrode using synchrotron spectroscopy, X-ray diffraction, high-resolution electron microscopy, electron diffraction and solid-state NMR spectroscopy. In this study, since there was no evidence of a special decomposition peak at the $LiCoO_2$ electrode, the discussion on the formation of the SEI layer at this electrode is still a matter of intense investigation. In the case of the graphite electrode, the special peak that is responsible for the formation of the SEI layer was shifted to the Li^+ reduction potential with a gradual increase in the concentration of $LiPF_6$. However, this phenomenon was dismissed as a minor occurrence, since the shift in the reduction potential was not large compared to the shift of the peak in the case of mixed-salt experiments. In the authors' previous paper on the mixed-salt effect due to the formation of the SEI layer, the reduction peak on the graphite electrode formed during the first charging period was confirmed as a valid peak, and it significantly affected the battery performance (i.e. charge/discharge capacities, life cycle, safety, and storage properties of the battery at high temperature) [18].

The faradaic currents increased dramatically from +0.5 and −2.5 V in the oxidation and reduction processes, respectively; these currents are probably attributable to the Li^+ dissociation from $LiCoO_2$ and Li^+ intercalation to graphite, and not to the electrochemical reaction of the electrolyte at the interface. Although there is no special peak assumed for the decomposition of the electrolyte, it is still regarded as a part of the faradaic reaction because the Li^+ ions are dissociated from $LiCoO_2$ by oxidation and intercalated to graphite by reduction in these regions. Note that the currents generated during the faradaic reactions decrease with an increase in the salt concentration, as shown in Fig. 1. Several reports on the relationship between the salt concentration and the ionic conductivity exist; a majority of these studies investigate how ionic conductivity can be increased or how the potential window can be expanded [19, 20]. For example, at low salt concentrations, the number of free ions increases with the salt concentration; consequently, the ionic conductivity also increases until a threshold concentration level is reached. Beyond this threshold, an increase in the salt concentration results in high ion aggregation and high solution viscosity, which simultaneously reduces the number and mobility of the free ions. These phenomena were investigated as the relationship between the lithium salt concentration and the faradaic currents in this study. The faradaic currents decreased with increase in the concentration of $LiPF_6$ over the potential ranges of +0.5 V at the $LiCoO_2$ and −2.5 V at graphite electrodes, respectively. This implies that it is not desirable to increase the salt concentration for developing an electrolyte system with high ionic conductivity, since a high salt concentration causes the ion aggregation and electrolyte viscosity to increase and disturb the mobility of Li ion. In addition, since the faradaic current generated by interaction of the Li^+ ion is closely related to the charging rate, this method provides useful information for preparing an optimal electrolyte for a Li ion battery used in hybrid electric vehicles (HEVs), which have high power requirements.

The amount of faradaic currents was reanalyzed to investigate the effects of salt concentration under a fixed potential condition, as shown in Fig. 2. The compared potentials were +1.5 V in the oxidation region and −3.5 V in the reduction region, which were the respective fully charged potentials of the $LiCoO_2$ anode and the graphite cathode. Redox currents were constant until the salt concentration reached 1.0 mol L^{-1}; then the currents decreased rapidly with increase in salt concentration. Since the amount of faradaic current generated depends on the amount of Li^+ ions dissociated from $LiCoO_2$ and intercalated to graphite in the Li ion battery, these experimental results show that 1.0 mol L^{-1} of $LiPF_6$ is a necessary and sufficient condition in this battery system. In other words, it is futile to increase the salt concentration above 1.0 mol L^{-1} even if the ionic conductivity increases. The reason for the above mentioned phenomena can be

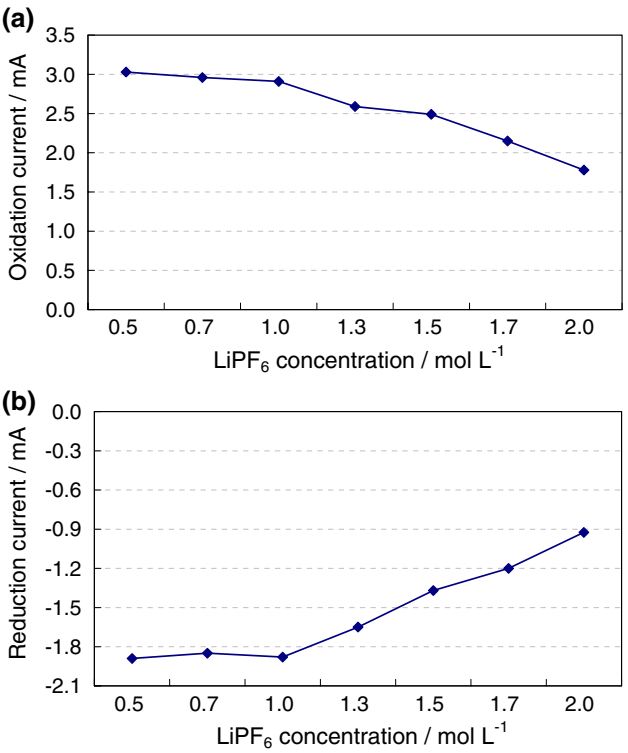

Fig. 2 Redox currents at the fixed potentials: **a** oxidation current at +1.5 V at $LiCoO_2$ anode, **b** reduction current at −3.5 V at the graphite cathode

explained in terms of the colligative properties of electrolyte solutions, such as ionic aggregation and electrolyte viscosity. These properties increase rapidly at a salt concentration greater than 1.0 mol L^{-1}.

3.2 Effect of solvent composition

To determine the electrolyte condition with the higher faradaic current at the graphite electrode during the charging period, the reduction current at −3.0 V was investigated using three different linear carbonates (DMC, EMC, and DEC) and EC. The concentration of $LiPF_6$ was fixed at 1.0 mol L^{-1}. As shown in Fig. 3, the reduction current increased dramatically from 20 vol.% of EC in all the three linear carbonate systems; it also increased in the descending order of DMC, EMC, and DEC. From these results, it was clear that the charging current increased with increase in the dielectric constant of the mixed solvent system; the dielectric constant of each solvent was EC (95), DMC (3.12), EMC (2.9), and DEC (2.82). However, the variation in the total dielectric constants of the mixed electrolyte systems was not sufficiently large to overcome the difference in the value of the currents generated in each system. In the case of the 50 vol.% EC system, the total dielectric constants calculated were 49.06, 48.95, and 48.91 for DMC, EMC and DEC system, respectively. The difference in the amounts of current generated can also be attributed to the presence of bulky solvent molecules. The molecular sizes of DMC (247.5 cm^3 mol^{-1}), EMC (303.5 cm^3 mol^{-1}), and DEC (395.5 cm^3 mol^{-1}) systems were calculated using Chem3D Pro 10.0. The current was inversely proportional to the molecular size of the linear carbonate. From these results, the faradaic currents generated by the Li^+ dissociation from $LiCoO_2$ and the Li^+ intercalation to graphite are shown to be directly proportional to the dielectric constant and inversely proportional to the degree of bulkiness of the solvent molecules.

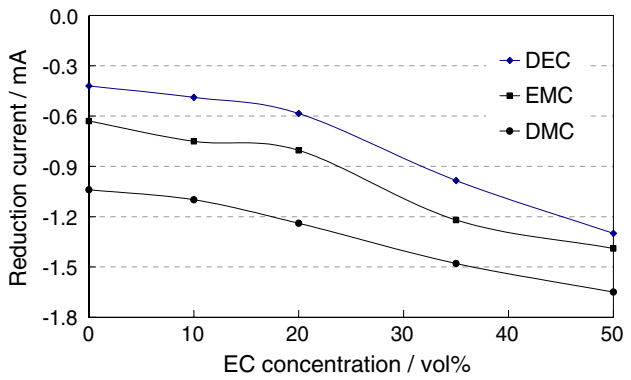

Fig. 3 Reduction currents at −3.0 V in the graphite with the EC concentration combined with three different linear carbonates

3.3 Effect of electrolyte salt

In general, ionic conductivity is defined in the same way as electronic conductivity

$$\sigma = nZe\mu \tag{1}$$

where n is the number of charge carriers per unit volume, Z is the charge of the ion, e is the elementary charge (1.602×10^{-18} C), and μ is the electrical mobility of the ionic species. The mobility of an ion is known to vary inversely with its radius r_i according to the Stokes–Einstein relation, which is expressed as follows [8]:

$$\mu = \frac{1}{6\pi\eta r_i} \tag{2}$$

where η is the viscosity of the media. Therefore, the ionic conductivity can be expressed as

$$\sigma = \frac{nZe}{6\pi\eta r_i} \tag{3}$$

In the Li ion battery, the ionic conductivity of the electrolyte is derived from the electrical mobility of the Li^+ ions. However, since the viscosity of the electrolyte solution is affected by the degree of bulkiness of the solvent molecules or the ionic bonding force of the salt, the counterparts of the Li^+ ions must also be considered. According to Ue's study on the ionic conductivity of various solvents, excellent conductivity can be obtained by a combination of the ionic mobility of the solvent and its dissociation constant [21]. In this study, the amount of faradaic current in the charging period was also investigated for the three kinds of lithium salts ($LiPF_6$, $LiBF_4$, and LiTFSI) under various solvent combinations. As shown in Fig. 4, the reduction current at −3.0 V decreased in the descending order of $LiPF_6$, LiTFSI, and $LiBF_4$ in the electrolyte systems. Since the ionic bonding force of $LiBF_4$ is stronger than that of $LiPF_6$ or LiTFSI [18], the number of dissociated Li^+ ions from $LiBF_4$ decreases in the EMC or the DEC system. The reduction current, generated by the intercalation of Li^+ ions to the graphite electrode, is affected by the dissociated ions from the $LiCoO_2$ electrode during the charging period. This current generated in the single linear carbonate system increased in the descending order of DMC, EMC, and DEC. And the current at −3.0 V was three times greater in DMC than that in the DEC system, in the case of $LiPF_6$. These results show that Li^+ ions were significantly intercalated to the graphite in the electrolyte system with $LiPF_6$ and DMC.

During the charging period of the Li ion battery, the non-faradaic current is generated from the capacitive components of the electrodes, and the faradaic current is mainly derived by the Li^+ interaction with the electrodes.

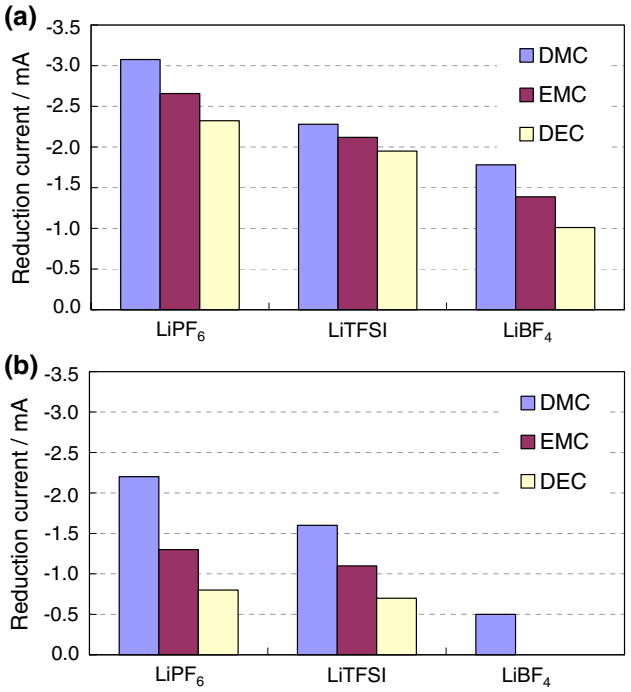

Fig. 4 Reduction currents measured at −3.0 V: **a** in the mixture of EC 50 vol.% and linear carbonate 50 vol.%, **b** in only linear carbonate (DMC, EMC, DEC)

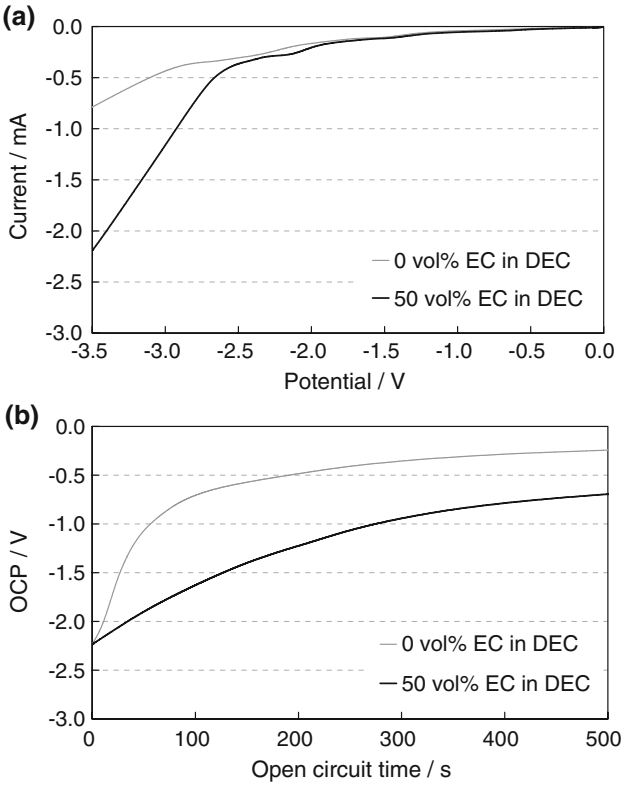

Fig. 5 Comparison of the open circuit potential (OCP) of the charged electrode: **a** charge profiles of graphite anode, **b** OCP profiles after charging to −3.5 V

And the rate of increase of electrode potential by the faradaic current is much slower than that by the non-faradiac current. These phenomena were verified by the OCP of the graphite electrode, as shown in Fig. 5. The OCP in a 100 vol.% EMC system was found to decrease more rapidly than that in a 50 vol.% EC-added system. These results indicate that more Li^+ ions were intercalated into the graphite electrode in the 50 vol.% EC-added systems than those in the 100 vol.% DEC system. And the increasing quantity of the potential of the graphite electrode by the Li^+ intercalation decreased under the 100 vol.% DEC system. In this study, the voltage-current profile was analyzed to determine the optimal electrolyte composition by comparing the faradaic current under different concentrations of $LiPF_6$, solvent component and salt type. Although these results are similar to the general studies, the method proposed here is suitable for preparing an optimal electrolyte for a real battery system.

4 Conclusions

In this paper, the faradaic and non-faradaic reactions during the charging period were investigated in order to determine an optimal electrolyte composition for an actual Li ion battery. The reactions were dependent on the composition of the electrolyte and were analyzed in terms of the faradaic and non-faradaic currents. Actually, the faradaic currents were associated with the concentration of $LiPF_6$ over the potential ranges of +0.5 V at the $LiCoO_2$ and −2.5 V at graphite electrodes, respectively. The faradaic current was also shown to be directly proportional to the dielectric constant and inversely proportional to the degree of bulkiness of the solvent molecules. And finally, the OCP of the electrode with a greater faradaic current decreased at a slower rate than that of the electrode with a smaller faradaic current. This analysis method can be used effectively for designing an optimal electrolyte system of an actual battery with excellent high-rate discharge capabilities and low temperature discharge properties.

Acknowledgements This study was supported by the Research Fund provided by the University of Seoul (2007-04271054). Preliminary experiments by Mr. Wonkyun Lee are acknowledged.

References

1. Xu K, Ding S, Jow TR (1999) J Electrochem Soc 146:4172
2. Guyomard D, Tarascon JM (1992) J Electrochem Soc 139:937
3. Ein-Eli Y, McDevitt SF, Aurbach D et al (1997) J Electrochem Soc 144:L180
4. Aurbach D, Ein-Eli Y (1995) J Electrochem Soc 142:1746

5. Bar-Tow D, Peled E, Burstein L (1999) J Electrochem Soc 146:824
6. Peled E, Bar Tow D, Merson A et al (2001) J Power Sources 97:52
7. Peled E, Menachem C, Bar-Tow D et al (1996) J Electrochem Soc 143:L4
8. Bard AJ, Faulkner LR (2000) Electrochemical methods fundamentals and applications, 2nd edn. Wiley, New York
9. Aurbach D, Levi MD, Levi E et al (1998) J Electrochem Soc 145:3024
10. Aurbach D, Gamolsky K, Markovsky B et al (2000) J Electrochem Soc 147:1322
11. Eriksson T, Andersson AM, Bishop AG et al (2002) J Electrochem Soc 149:A69
12. Andersson AM, Abraham DP, Haasch R et al (2002) J Electrochem Soc 149:A1358
13. Novak P, Panitz J-C, Joho F et al (2000) J Power Sources 90:52
14. Balasubramanian M, Sun X, Yang XQ et al (2001) J Power Sources 92:1
15. Teradaa Y, Yasakaa K, Nishikawab F et al (2001) J Solid State Chem 156:286
16. Meng YS, Ceder G, Grey CP et al (2004) Electrochem Solid State Lett 7:A155
17. Grey CP, Dupr'e N (2004) Chem Rev 104:4493
18. Jung C (2008) Solid State Ionics 179:1717
19. Ue M, Murakami A, Nakamura S (2002) J Electrochem Soc 149:A1572
20. Wang S, Qiu W, Guan Y et al (2007) Electrochimica Acta 52:4907
21. Ue M (1994) J Electrochem Soc 141:3336